Journal of Nanobiotechnology

RESEARCH

Open Access

Autologous platelet delivery of siRNAs by autologous plasma protein self-assembled nanoparticles for the treatment of acute kidney injury

Jiafan Wang[1†], Hai Huang[2†], Meng Jia[1†], Si Chen[3†], Fengjuan Wang[1†], Guiyang He[1], Chong Wu[1], Kaibin Lou[1], Xuexue Zheng[1], Heng Zhang[1], Chao Qin[4*], Yanggang Yuan[3*], Ke Zen[1,5*] and Hongwei Liang[1*]

Abstract

Acute kidney injury (AKI) involves the activation of intrarenal hemostatic and inflammatory pathways. Platelets rapidly migrate to affected sites of AKI and release extracellular vesicles (EVs) laden with bioactive mediators that regulate inflammation and hemostasis. While small interfering RNA (siRNA) is a potent gene-silencing tool for biomedical applications, its therapeutic application in vivo remains challenging. We developed an innovative nucleic acid delivery platform by hybridizing synthetic transformation-related protein 53 (p53) siRNA with autologous plasma and incubating the complex with autologous platelets. These engineered platelets selectively delivered p53 siRNA to injured renal tubular cells via EV-mediated cargo release, resulting in targeted p53 suppression in renal cells and subsequent attenuation of AKI progression. This platelet-centric translational strategy demonstrates significant potential for advancing precision therapies in AKI by exploiting endogenous platelet trafficking to deliver therapeutics directly to injury sites.

Keywords Acute kidney injury, Platelets, Self-assembling nanoparticles, Transformation-related protein 53

[†]Jiafan Wang, Hai Huang, Meng Jia, Si Chen and Fengjuan Wang contributed equally to this work.

*Correspondence:
Chao Qin
qinchao@njmu.edu.cn
Yanggang Yuan
ygyuan@njmu.edu.cn
Ke Zen
kzen@nju.edu.cn
Hongwei Liang
hwliang@cpu.edu.cn

[1]Department of Emergency, School of Life Science and Technology, Nanjing Drum Tower Hospital, China Pharmaceutical University, Nanjing, China
[2]Department of Endocrinology and Metabolism, the First Affiliated Hospital of Nanjing Medical University, Nanjing, Jiangsu, China
[3]Department of Nephrology, The First Affiliated Hospital of Nanjing Medical University, Nanjing, China
[4]Department of Urology, The First Affiliated Hospital of Nanjing Medical University, Nanjing 210029, China
[5]State Key Laboratory of Pharmaceutical Biotechnology, School of Life Science, Nanjing University, Nanjing, China

Introduction

Acute kidney injury (AKI), which is characterized by an abrupt decline in renal function, poses a substantial clinical burden with high morbidity and mortality worldwide, afflicting over 13 million patients annually and causing ~ 2 million fatalities [1]. This heterogeneous syndrome arises from diverse insults, including nephrotoxic, ischemic, and septic injuries [1, 2], and is associated with a significant risk of progression to chronic kidney disease and end-stage renal failure [1]. Despite advances in elucidating AKI pathophysiology, therapeutic options remain limited to supportive care modalities such as dialysis or transplantation, interventions burdened by cost-prohibitive expenses and persistently poor survival outcomes [1]. The absence of targeted pharmacotherapeutics underscores the critical unmet need for mechanism-driven AKI therapies.

RNA interference (RNAi), a conserved eukaryotic mechanism, uses sequence-specific small interfering RNAs (siRNAs) to silence genes through complementary mRNA degradation [3]. This process has emerged as a transformative therapeutic strategy for selectively suppressing pathogenic gene expression [3]. However, the clinical translation of RNAi faces a critical bottleneck: siRNA must evade systemic clearance and degradation to reach cytoplasmic targets intact [3]. Current efforts prioritize the development of efficient, tissue-specific delivery systems [3]. While viral vectors achieve high transfection efficiency, their clinical utility is limited by their cytotoxicity, oncogenic potential, and immunogenicity [4]. Nonviral alternatives, particularly nanoparticles, have gained traction because of their superior biocompatibility and safety profiles [4]. Engineered nanoparticles facilitate nucleic acid delivery through membrane penetration [5], offering advantages such as low cytotoxicity, robust cellular uptake, and high transfection efficiency [6–8]. These attributes have spurred their widespread adoption across pharmaceuticals, biomedical engineering, and industrial applications [8–10]. Nevertheless, nanoparticle-based delivery systems face limitations, including poor colloidal stability, nonspecific biodistribution, accelerated reticuloendothelial clearance, residual immunogenicity, and suboptimal targeting precision [11].

Emerging strategies leveraging living cell-mediated delivery, particularly platelet-based systems, may circumvent these challenges [12]. Platelets, the second most abundant type of circulating blood cell (150–400 × 109/L), constitute ~ 5% of total body cells [13]. Under physiological conditions, platelets maintain a quiescent, nonadherent state through endothelial-derived inhibitory signals [14]. In AKI, however, endothelial dysfunction disrupts these regulatory mechanisms, exposing platelets to activating stimuli [14]. Activated platelets rapidly home to injury sites via adhesion molecule- and chemokine-mediated interactions, forming aggregates within damaged renal tissue. At these sites, platelets release soluble mediators and extracellular vesicles (EVs) carrying bioactive cargo (proteins, nucleic acids, and lipids) that orchestrate tissue repair [14]. Platelet-derived EVs enhance renal recovery by promoting endothelial proliferation, tubular cell survival, and immunomodulation, thereby fostering a regenerative microenvironment [14]. These observations have spurred interest in platelet EV-based or platelet membrane-biomimetic nanoparticles for targeted renal therapy [15–17]. However, current EV engineering approaches require synthetic polymer encapsulation of siRNAs, which introduces procedural complexity and risks of polymer-associated cytotoxicity. Furthermore, EV isolation or platelet membrane extraction may induce unintended platelet activation or lysis, potentially exacerbating coagulation disorders. These technical and safety hurdles currently preclude rapid clinical translation for AKI treatment.

Preclinical studies have identified multiple siRNA targets with therapeutic potential in AKI, including Arg-2 siRNAs [18], PHD2 siRNAs [19], TLR9 siRNAs [20], Mep1 siRNAs [21] and Trp53 siRNAs [21–27]. Among these proteins, p53 (transformation-related protein 53) has emerged as a central regulator of AKI pathogenesis and postinjury repair dynamics [1, 28]. The upregulation of p53 in tubule cells is a pivotal response to cellular stressors such as DNA damage, hypoxia, and the generation of reactive oxygen species [1]. Pifithrin-α, a p53 inhibitor, can mitigate tubule apoptosis and restore renal function [29]. However, its precise molecular mechanism remains incompletely understood, as it inhibits only certain aspects of p53 function. In contrast, intravenous injection of synthetic siRNAs targeting p53 appears to offer more precise and comprehensive protection of tubule cells, contributing to the restoration of renal function [27]. Nevertheless, despite their natural tendency to target the kidneys, free siRNA faces several pharmaceutical challenges in treating acute kidney injury (AKI). The macromolecular nature and strong negative charge of siRNA make it difficult for it to cross cell membranes and reach its site of action in the cytoplasm [27]. Consequently, large amounts of free siRNA might need to be administered through a "hydrodynamic" dosing method to achieve the desired gene silencing effect in the kidneys [27]. Moreover, as a potent stimulator of the innate immune system, high doses of synthetic siRNA can lead to adverse immunostimulatory effects [30].

We previously demonstrated that synthetic small RNAs can rapidly self-assemble into nanoparticles in the presence of serum through phase separation, thereby enabling their entry into various cell types [31]. In the present study, we further confirmed that synthetic siRNAs can similarly self-assemble into approximately

150 nm nanoparticles in the presence of plasma, facilitating their entry into platelets. By leveraging this approach, we developed a novel siRNA delivery system that utilizes autologous proteins and platelets for the treatment of AKI. Specifically, p53 siRNAs were first encapsulated within nanoparticles via autologous plasma proteins and then incorporated into autologous platelets. These engineered platelets exhibit intrinsic homing to renal injury sites, where they release p53 siRNA via platelet-derived EVs, mediating targeted p53 protein knockdown and subsequent attenuation of tubular damage. In conclusion, we have established a clinically translatable, platelet-mediated siRNA delivery platform that achieves targeted renoprotection with negligible systemic toxicity. This system holds promise as a novel bedside therapeutic strategy for AKI.

Materials and methods

Materials

The cyanine 5 (Cy5)-labeled (the cyanine 5 fluorophore attached at the 5′-terminus) or naked scramble RNA (siRNA-NC), TP53 siRNA and Trp53 siRNAs (siRNA-Trp53) were 2′-O-methylated and synthesized by GenScript (Nanjing, China). The reverse complementary sequence of siRNA-TP53 (siRNA-TP53 inhibitor) was synthesized by GenePharma (Shanghai, China). Cisplatin (CDDP) was obtained from TargetMol Chemicals, Inc. (Boston, USA). GW4869 was purchased from MedChemExpress (MCE, HY-19363). To collect EV-free fetal bovine serum (EV-free FBS) and EV-free plasma, the FBS (Gibco, 10099141 C) and plasma were centrifuged at 3000 × g for 30 min and filtered through 0.45 μm filters (Millipore, HAWP04700), followed by a second spin at 10,000 × g for 30 min and a final high-speed spin at 100,000 × g for 70 min [32].

Cell culture and CDDP treatment

Human renal tubular epithelial cells (HK-2 cells) were purchased from the American Type Culture Collection (Rockville, MD, USA) and cultured in DMEM/F-12 medium (DF/12, Gibco, Grand Island, USA) supplemented with 1% antibiotics (penicillin and streptomycin, P/S, Gibco) and 10% EV-free FBS. To induce damage in HK-2 cells, HK-2 cells were cultured in complete DMEM/F-12 supplemented with 10% EV-free FBS and CDDP (the final concentration of CDDP was 20 μM) for 12 h. The cells utilized in this experiment were maintained at 37 °C and 5% CO_2.

Platelet isolation

The whole blood of the mice or healthy human volunteers was collected in EDTA Vacutainer® tubes (BD, Franklin Lakes, USA) and centrifuged at 300 ×g for 20 min. The cell pellet was discarded, and the upper solution was composed of platelet-rich plasma. The platelet-rich plasma was then further centrifuged at 3000×g for 15 min, and the resulting cell precipitate was composed of platelets and erythrocytes. The platelet-free plasma was subsequently carefully extracted and stored at 4 °C in a 1.5 mL RNase-free tube. The precipitate was subsequently resuspended in precooled red blood cell lysis buffer (420301, BioLegend, San Diego, CA) and incubated on ice for 5 min to eliminate red blood cells. Afterward, the mixture was centrifuged at 3000×g for 10 min to isolate the platelets. The platelets in the precipitate were resuspended in aseptic normal saline and stored at 4 °C.

Characterization of the nanoparticles formed by synthetic SiRNAs and plasma

To investigate the nanoparticles formed by synthetic siRNAs and plasma, 1 ml of EV-free plasma was mixed with 0.5 pmol siRNA-Trp53 at room temperature for 5 min. The mixture was then diluted with PBS to reduce the plasma proportion to 10% prior to analysis by nanoparticle-tracking analysis (NTA) and transmission electron microscopy (TEM) in accordance with previously reported methods [33]. The zeta potential of the self-assembled siRNA nanoparticles was determined via a Zetasizer NanoZS (Malvern Instruments, UK).

Mass spectrum

Five milliliters of EV-free plasma was combined with 2.5 pmol synthetic siRNA-Trp53 for 10 min at room temperature. The mixture was then diluted with 5 ml of PBS. A control group was established by diluting 5 ml of EV-free plasma with 5 ml of phosphate-buffered saline (PBS). All the groups were centrifuged at 120,000×g for 2 h, after which the sediment was resuspended in 100 μl of sterile PBS for protein mass spectroscopic analysis via LC–MS/MS.

Preparation of SiRNA (cy5-tagged or naked)-loaded platelets

One milliliter of EV-free plasma was incubated with 0.5 pmol of synthetic siRNA-Trp53 (either Cy5-labeled or unlabeled) at room temperature for 10 min to facilitate nanoparticle formation. Next, 10^8 freshly isolated platelets were combined with the nanoparticles and gently rotated to ensure thorough mixing. The mixture was then centrifuged at 3,000×g for 10 min. The resulting pellet was washed twice with PBS to yield platelets loaded with siRNA.

Simultaneous measurement of platelet aggregation and dense granule secretion

The aggregation of platelets and dense granules release were assessed simultaneously via a luminometer (Chrono-log model 700). Aggregation curves were

obtained as a function of increasing light transmittance through stirred PRP samples during platelet aggregation. During the same analysis, the ATP release from dense platelet granules from the samples was measured. A high-gain photomultiplier recorded the light emitted during the reaction between platelet-secreted ATP and the firefly luciferin-luciferase mixture (chronolume reagent), which was proportional to the amount of secreted ATP (expressed in nanomoles) following the addition of the stimulator. Aggregation and secretion were triggered by collagen (2 μg/ml final conc., Chronopar reagent).

Flow cytometry of the activated platelet marker CD62P and integrin AIIbβ3

Human platelets were stimulated with thrombin (0.01 U/mL). PE-conjugated CD62P (P-selectin) antibody (Invitrogen, 12-0626-82) and GPIIb/IIIa (integrin αIIbβ3) antibody (Abnova, MAB5226) were used for labeling. The mean fluorescence intensity (MFI) was measured via flow cytometry (BD Biosciences), and the data were analyzed via FlowJo v10 software.

Coculture of HK-2 cells and platelets

For confocal fluorescence imaging, 4×10^6 Cy5-labeled siRNA-Trp53-loaded platelets were incubated with 1×10^4 HK-2 cells in a 12-well plate at room temperature for 12 h. After incubation, the platelets were removed by washing the cells twice with PBS. The HK-2 cells were then stained with DAPI and imaged via laser scanning confocal microscopy. For Western blotting and RT–qPCR, 4×10^6 platelets loaded with siRNAs were cocultured with 1×10^4 HK-2 cells. In the CDDP-treated group, HK-2 cells were pretreated with 10 nM CDDP for 24 h prior to coculture with platelets. Before RNA and protein were extracted from HK-2 cells for Western blotting and RT–qPCR, the cells were rinsed twice with PBS to remove any residual platelets. Similarly, for the functional assay in the CDDP-treated group, HK-2 cells were pretreated with 10 nM CDDP for 24 h before being cocultured with platelets. To verify that Trp53-siRNA was delivered into HK-2 cells via EVs, 4×10^6 platelets were first treated with GW4869 (final concentration of 5 μmol/L) for 24 h. Subsequently, the platelets were incubated with nanoparticles formed by Trp53 siRNAs in the presence of EV-free plasma for 4 h to collect the pretreated platelets. HK-2 cells (1×104) were treated with or without CDDP for 24 h. Then, the pretreated platelets were cocultured with HK-2 cells for 24 h, and the Trp53 protein levels were investigated via western blotting, and the cell viability was determined via a CCK-8 assay.

Collection and characterization of platelet-derived EVs

HK-2 cells (5×10^3) were initially treated with or without 20 μM cisplatin (CDDP). Twelve hours later, the CDDP-containing medium was replaced with Dulbecco's modified Eagle's medium (DMEM) supplemented with 10% EV-free plasma. Twenty-four hours later, 10 mL of the cell culture medium from the HK-2 cells previously treated with or without 20 μM CDDP was collected and subjected to sequential centrifugation at 3,000×g for 30 min at 4 °C. The samples were then subjected to centrifugation at 10,000×g for 30 min at 4 °C, followed by centrifugation at 100,000×g for 70 min at 4 °C in accordance with a previously reported protocol [33]. EV-free cell culture medium was incubated with freshly separated platelets (5×10^6/ml) at 37 °C and 5% CO_2 for 48 h. The medium was subsequently collected and subjected to centrifugation at 3,000×g for 30 min at 4 °C to remove the platelets, 10,000×g for 30 min at 4 °C to remove the cell debris, and 100,000×g for 70 min to collect the EVs released by the platelets, as previously described in a published report [33]. The EVs released by the platelets were examined via transmission electron microscopy (TEM), nanoparticle tracking analysis (NTA), western blotting or RT–qPCR in accordance with previously reported methods [33].

RNA extraction and reverse transcription quantitative PCR (RT–qPCR)

For the detection of mRNA, total RNA was extracted via TRIzol™ reagents (Invitrogen, 15596026) in accordance with the manufacturer's instructions. cDNA was subsequently synthesized with the HiScript II 1st Strand cDNA Synthesis Kit (Vazyme, R212). Real-time qPCR (RT–qPCR) was carried out via the ChamQ Universal SYBR qPCR Master Mix Kit (Vazyme, Q711). For siRNA detection, RNA was extracted via RNAiso for small RNA reagents (Takara, 9753). A MiRNA 1st Strand cDNA Synthesis Kit (Vazyme, MR101) was used for miRNA reverse transcription. cDNA synthesis was conducted for 15 min at 50 °C, and the reaction was terminated by heating at 85 °C for 5 min. Real-time quantitative polymerase chain reaction (qPCR) was then conducted with the miRNA Universal SYBR qPCR Master Mix Kit (Vazyme, MQ101). Two microliters of cDNA was subjected to 40 cycles of 95 °C for 10 s and 60 °C for 30 s on an ABI 7500 Fast Real-Time PCR System (Thermo Fisher Scientific). The absolute quantitative calculation of siRNA was conducted in accordance with the provided operating instructions [31]. Briefly, siRNAs (1, 0.5, 0.25, 0.05, or 0.01 pmol) were dissolved in 1 ml of PBS, and total RNA was extracted from the mixture for qRT–PCR. A linear curve between the C_T value and the absolute number of corresponding siRNAs was drawn to calculate the number of siRNAs in the solution. The primers used are listed in Table S1.

Western blot

The cells and tissues were harvested with radioimmunoprecipitation assay buffer (RIPA buffer) (R0278, Merck), and the cell debris was depleted after centrifugation at 12,000×g at 4 °C. The supernatant was boiled at 100 °C for 5 min before being loaded onto a 10% polyacrylamide gel. Proteins resolved by SDS–PAGE were transferred onto polyvinylidene fluoride membranes. The membranes were blocked for one hour and incubated with primary antibodies against Trp53 (1:2000, 2524; Cell Signaling Technology) and GAPDH (1:5000, G9295; Sigma–Aldrich) at 4 °C. The membranes were subsequently washed with Tris-buffered saline and Tween-20 (TBST) and incubated with a horseradish peroxidase (HRP)-conjugated secondary antibody (anti-mouse IgG, 1:2000, 7076; Cell Signaling Technology) at room temperature for 2 h. The luminosity of the protein bands was quantified and analyzed via ImageJ software (National Institutes of Health). To identify the markers of platelet-derived EVs, the platelet-derived EVs were lysed via radioimmunoprecipitation assay buffer (RIPA buffer) (R0278, Merck), and western blotting was performed with anti-CD63 (Cell Signaling Technology, 10112 S), anti-TSG101 (Proteintech, 28283-1-AP), and anti-ALIX (Abcam, ab117600) antibodies as previously reported [32].

Cell counting Kit-8 (CCK-8) assay

HK-2 cells (1 × 104) were treated with or without CDDP for 12 h. Then, 4×10^6 platelets were incubated with the HK-2 cells. After 24 h, cell viability was determined with a Cell Counting Kit-8 (CCK-8, Yeasen) in accordance with the manufacturer's instructions. To assess the protective effect of siRNA-Trp53-loaded platelet-derived EVs on HK-2 cells against CDDP-induced toxicity, 8×10^2 HK-2 cells were seeded in a 96-well plate. Subsequently, the HK-2 cells were treated with or without CDDP for 12 h. Then, 0.5 μg (total protein) of platelet-EVs was incubated with the HK-2 cells. After 24 h, cell viability was determined with a Cell Counting Kit-8 (CCK-8, Yeasen) in accordance with the manufacturer's instructions. To identify the protective effect of siRNA-Trp53 on HK-2 cells derived from platelet-derived EVs, 8×10^2 HK-2 cells were seeded in a 96-well plate and transfected with a siRNA-Trp53 inhibitor. The HK-2 cells were then treated with or without 20 μM CDDP. Following a 12-h incubation period, 0.5 μg (total protein) of platelet-derived EVs were added to the HK-2 cells and incubated for an additional 24 h. Cell viability was then determined with a Cell Counting Kit-8 (CCK-8, Yeasen) in accordance with the manufacturer's instructions.

In vivo imaging

To demonstrate the distribution and efficacy of platelets in delivering drugs to injured kidneys, male C57BL/6 mice (8 weeks old) were purchased from GemPharmatech (Nanjing, China). Healthy C57BL/6 mice served as the control group. The acute kidney injury C57BL/6 mouse model was induced by ischemia–reperfusion or CDDP, as previously reported [34]. Briefly, for the ischemia–reperfusion model, 8-week-old male C57BL/6 mice were anesthetized with isoflurane and placed on a heated pad to maintain their body temperature at 37 °C. The bilateral renal vessels were occluded via nontraumatic microaneurysm clamps for 30 min via flank incisions. The incisions were subsequently sutured, and the mice were returned to their cages. For the CDDP-induced model, CDDP was dissolved in normal saline, sonicated for 20 min, and chilled on ice. All the mice received an intraperitoneal injection of 0.5 mg of CDDP per mouse. Following a two-day period of ischemia–reperfusion and CDDP treatment, the mice were administered Cy5-labeled siRNA-Trp53 or scramble RNA-loaded platelets (5×10^7 per mouse) via the tail vein. Twenty-four hours later, the mice were euthanized and perfused through the heart. The brain, heart, lung, liver, kidney, and spleen were collected. Ex vivo imaging was subsequently conducted to capture and analyze the average number of photons per pixel per millisecond of the image. The renal tissues were further sectioned to observe the distribution of the siRNAs and platelets in the renal tissue via immunofluorescence staining via laser scanning confocal microscopy. An anti-CD41 antibody (ab33661, Abcam) was used to label platelets, and an anti-MCP-1 antibody (ab308522, Abcam) was used to label damaged renal tubular cells.

Therapeutic effect of platelets in vivo

To demonstrate the therapeutic effect of platelets in delivering drugs to injured kidneys, male C57BL/6 mice (8 weeks old) were purchased from GemPharmatech (Nanjing, China). Two acute kidney injury mouse models were induced via ischemia–reperfusion or CDDP, as previously reported [34]. The mice were randomly assigned to four groups: the siRNA-NC group, the siRNA-Trp53 group, the scrambled RNA group, and the siRNA-Trp53 group. The mice were grouped according to the injection schedule, with each mouse receiving 0.1 mg of naked siRNA [21] or 10^7 platelets injected through the tail vein every two days, for a total of four injections. Two days after the final injection, the serum was collected from the mice, and they were then euthanized to collect the kidneys and livers for western blotting and immunohistochemical staining to evaluate the therapeutic effect. At least five to six mice were included in each experimental group.

Quantification of BUN, creatinine and neutrophil gelatinase-associated Lipocalin

The urea nitrogen (BUN) levels were assessed via the DetectX Urea Nitrogen Detection Kit from Thermo Fisher Scientific (EIABUN), following the manufacturer's instructions. The serum creatinine levels were quantified with a creatinine assay kit from Nanjing JianCheng Bioengineering Institute (C011-2-1) in accordance with the provided protocol. The concentration of neutrophil gelatinase-associated lipocalin in the serum was determined via the Mouse NGAL ELISA Kit from Proteintech (KE10045) in accordance with the provided manual.

Tissue histology and immunostaining

The kidneys, livers and hearts were fixed in 4% paraformaldehyde solution and embedded in paraffin for hematoxylin and eosin (HE) staining. Renal tubular injury is characterized by tubular dilation, tubular atrophy, tubular cast formation, sloughing of tubular epithelial cells, loss of the brush border, and thickening of the tubular basement membrane. A scoring system was used as follows: a score of 0 indicated no tubular injury, whereas a score of 1.0, 1.5, 2.0, 2.5, 3.0, 3.5, 4.0, 4.5 and 5.0 represented 0–10%, 10–15%, 15–20%, 20–25%, 25–30%, 30–35%, 35–40%, 40–50% and >50% of tubules injured, respectively. The presence of myocardial injury in each AKI mouse model induced by IRI and CDDP was determined by examining the morphology of myocardial cells. For immunohistochemical (IHC) staining, the slides were incubated with primary antibodies against p53 (10442, Proteintech), Bax (14796, CST), Bcl2 (26593, Proteintech), and cleaved caspase 3 (9661, CST).

Statistical analysis

Each experiment was repeated a minimum of three times. Qualitative data, including histological images, represent findings from at least three independent experiments. All the statistical analyses were conducted via GraphPad Prism 8 software, and the results are presented as the means ± standard errors of the means (SEMs). Prior to analysis, all the data were assessed for a normal distribution and equal variance. Depending on the nature of the datasets, statistical comparisons were carried out via unpaired Student's t tests and one-way ANOVA. Statistical significance among groups was considered for values of $P < 0.05$. For the Western blot experiments, the statistical outcomes are presented after data normalization. This normalization process was implemented to reduce background variations arising from diverse experimental conditions. In this study, significance levels are denoted by *, **, and ***, representing $P < 0.05$, $P < 0.01$, and $P < 0.001$, respectively.

Results

Self-assembling SiRNA nanoparticles in the presence of plasma cationic proteins

As indicated in our previous study, synthetic small RNAs undergo serum-induced phase separation to form self-assembled nanoparticles [31], and we investigated whether analogous siRNA phase separation occurs in the presence of plasma. To test this hypothesis, synthetic TP53 siRNA was incubated with EV-free plasma, and nanoparticle assembly kinetics were quantified via NTA and TEM. NTA revealed rapid formation of nanoparticles (approximately 150 nm) when the siRNAs were exposed to EV-free plasma (Fig. 1a), in contrast with the negative controls, where neither the PBS-suspended siRNA nor the plasma alone produced detectable nanoparticles. TEM further confirmed the spherical morphology and size consistency (150 nm) of these assemblies (Fig. 1b). Crucially, these plasma-derived nanoparticles conferred significant siRNA stability, reducing RNase-mediated degradation (Figure S1a).

Prior studies have established that cationic polypeptides drive RNA nanoparticle assembly via phase separation [31, 35, 36]. To investigate whether endogenous cationic plasma proteins mediate TP53 siRNA nanoparticle formation, we isolated siRNA–protein complexes from EV-depleted plasma via 100 kDa centrifugal filtration and performed quantitative proteomic profiling via high-resolution LC–MS/MS. Proteomic analysis revealed that 84.79% of the nanoparticle-associated proteins were cationic (isoelectric points, pI > 7) (Fig. 1c; Supplementary Datasets S1), with cellular origin mapping via CIBERSORT [37] showing predominant contributions from T cells, monocytes, and mast cells (Fig. 1d; Supplementary Datasets S2). To functionally validate the cation dependency, we modulated the plasma pH (4–10) to titrate the protein surface charge–siRNA encapsulation efficiency inversely correlated with pH, which decreased 4000-fold from pH 4–10 (Fig. 1e). Consistent with our findings in serum [38], cationic protein depletion (achieved by heparin-affinity chromatography) in EV-depleted plasma completely abolished siRNA nanoparticle formation (Figure S1b-c). These results collectively demonstrate that charge-mediated protein–RNA interactions govern plasma-driven phase separation, with cationic immune cell-derived proteins serving as natural RNA condensing agents.

To determine the concentration-dependent relationship between EV-depleted plasma and siRNA nanoparticle assembly, TP53 siRNA was titrated against serial plasma dilutions (0–100% v/v). NPs were isolated via 100 kDa centrifugal filtration, and the partitioned siRNAs were quantified via RT–qPCR. As shown in Fig. 1f, the amount of nanoparticle-encapsulated siRNA increased proportionally with the plasma concentration, whereas

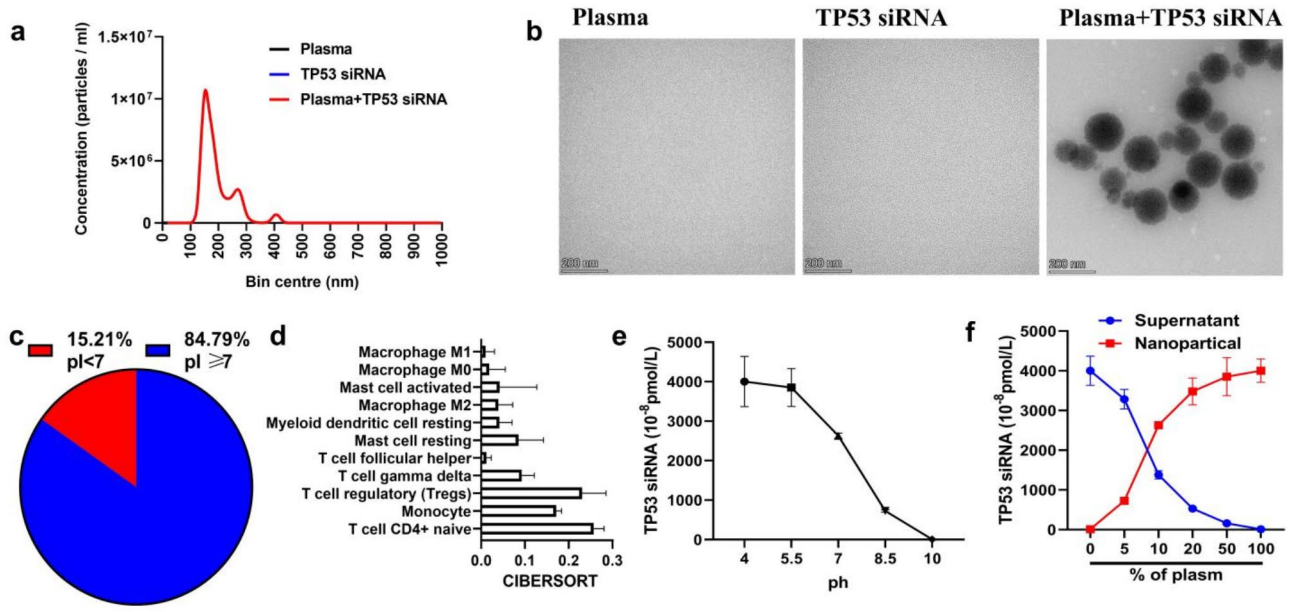

Fig. 1 Self-Assembling Nanoparticles composed of Autologous Plasma Proteins and siRNAs. (**a**) Formation of 150 nm siRNA nanoparticles after mixing with 10% EV-free plasma, as assessed via NanoSight. (**b**) TEM images of 10% EV-free plasma, 10% siRNA, and a mixture of siRNA and 10% EV-free plasma. Scale bar: 200 nm. (**c**-**d**) The isoelectric point distribution and cellular source of proteins forming nanoparticles with siRNA. (**e**) Nanoparticles formed from small RNA and plasma proteins at different pH values. (**f**) Nanoparticles formed from small RNA and plasma proteins at different proportions of plasma. The plasma was isolated from human blood

the amount of free siRNA in the filtrate decreased reciprocally, confirming plasma dependency. Under physiological pH (7.4) and 100% plasma, the optimized nanoparticles exhibited a 66.35% ± 0.16 encapsulation efficiency and 0.3318 pmol/(10^8 particle) loading capacity with a 6.33 mV ± 1.34 zeta potential. These parameters remained stable (> 90% retention) after 24 h, demonstrating formulation robustness.

Entry of SiRNA nanoparticles into platelets

Building on our previous discovery that serum-induced phase-separated small RNA nanoparticles enhance cellular internalization [31], we investigated whether plasma-protein/siRNA self-assemblies facilitate platelet transfection. Cy5-labeled TP53 siRNA was precomplexed with EV-depleted plasma (10 min, RT) and incubated with platelets (37 °C, 1 h). Confocal imaging revealed rapid cytosolic siRNA accumulation (Fig. 2a), which was corroborated by RT−qPCR quantification (Fig. 2b). The uptake kinetics of TP53 siRNAs and Mep1b siRNAs demonstrated temperature- and plasma-dependent internalization (Fig. 2, c-f). Notably, uptake was abolished at 4 °C (energy-dependent endocytosis) or in plasma-free conditions (Fig. 2, c-f), implicating phase-separated nanoparticles as obligate delivery vehicles. Crucially, nanoparticle-mediated siRNA loading did not alter platelet activation or function (e.g., the aggregation response) (Figure S2).

Platelets deliver TP53 SiRNA into renal tubule cells and protect them from CDDP-induced toxicity

To assess platelet-mediated siRNA delivery and subsequent gene silencing in renal tubule cells, siRNA-loaded platelets were cocultured with HK-2 cells (Fig. 3a). Confocal microscopy confirmed the efficient transfer of Cy5-labeled TP53 siRNA from platelets to HK-2 cells (Fig. 3b). Quantitative RT−qPCR analysis demonstrated successful delivery of TP53 siRNA from platelets to HK-2 cells (Fig. 3c).

Cisplatin (CDDP) exposure induced HK-2 cell death by upregulating TP53 expression (Figure S3a) [2, 22, 27, 28]. The efficacy of TP53 siRNA in reducing TP53 protein levels was validated by direct transfection via Lipofectamine 3000 (Figure S3b-e). TP53 protein levels were significantly elevated in HK-2 cells treated with CDDP (Figure S3d-e), and TP53 knockdown via direct siRNA transfection rescued CDDP-induced cell death (Figure S3f). Notably, the transfer of TP53 siRNA from platelets to HK-2 cells was significantly greater in the presence of CDDP than in the absence of CDDP (Fig. 3c). The incubation of HK-2 cells with platelets loaded with siRNA-TP5 significantly reduced TP53 protein levels (Fig. 3d) and attenuated CDDP-induced cell death (Fig. 3e).

EVs released by platelets transfer TP53 SiRNA into renal tubular cells

Activated platelets are known to secrete high levels of cytokines, chemokines, immunoglobulins, and EVs,

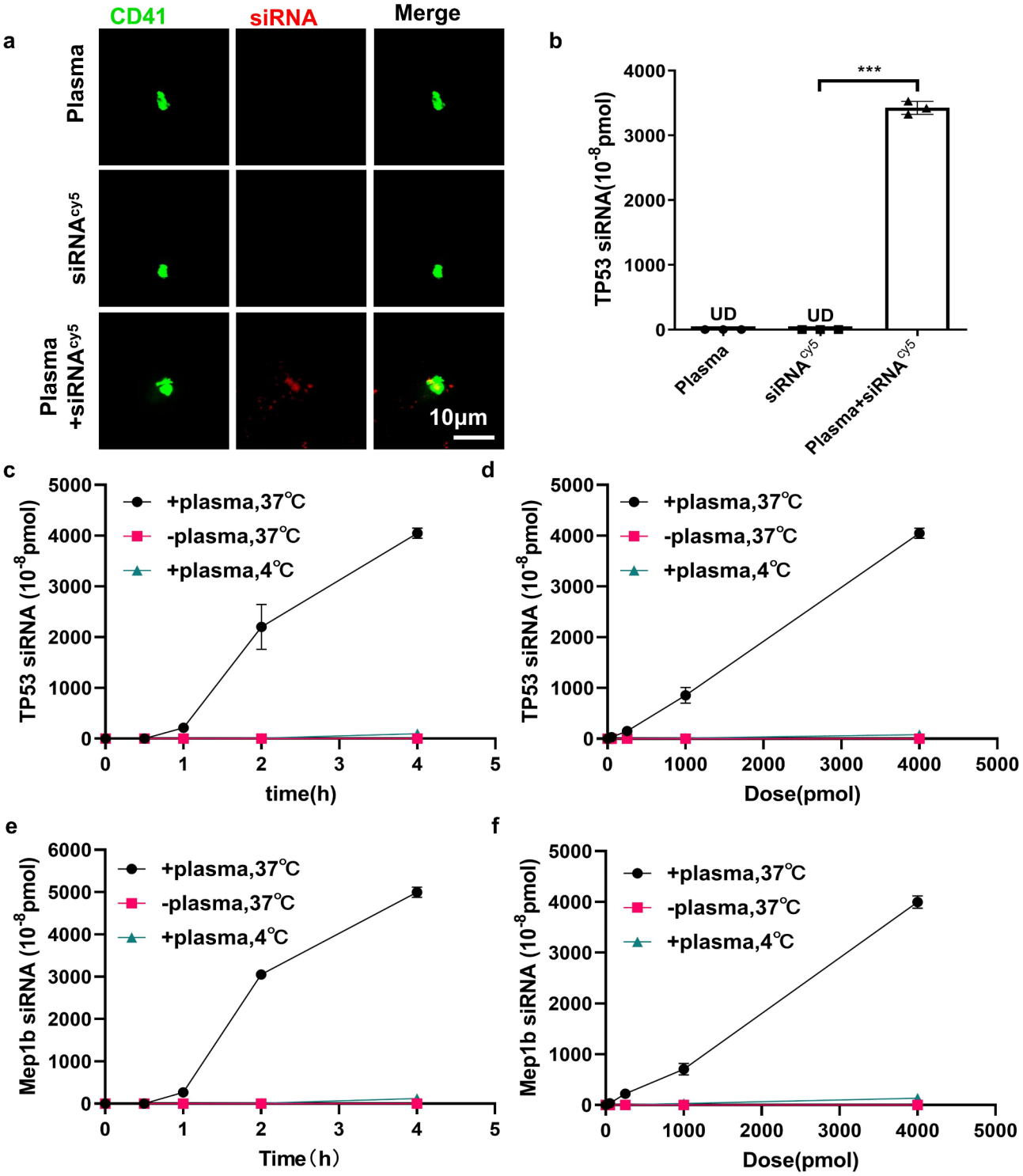

Fig. 2 Direct uptake of siRNAs by platelets in the presence of plasma. (**a**-**b**) Uptake of 0.5 fmol of Cy5-siRNA by platelets under various conditions. a: Representative image (scale bar: 10 μm); b: quantification of Cy5-siRNA uptake by 10^5 platelets subjected to various treatments. The plasma and platelets were isolated from human blood. (**c**-**d**) Time course and dose course of 0.5 fmol Trp53 siRNA taken up by 10^5 platelets under various conditions. The plasma and platelets were isolated from human blood. (**e**-**f**) Time course and dose course of 0.5 fmol Mep1b siRNA taken up by 10^5 platelets under various conditions. The plasma and platelets were isolated from mouse blood. Each experiment was repeated three times. Statistical differences between groups were assessed by independent-samples *t* tests. UD: undetected. Data with a P value < 0.05 were considered statistically significant

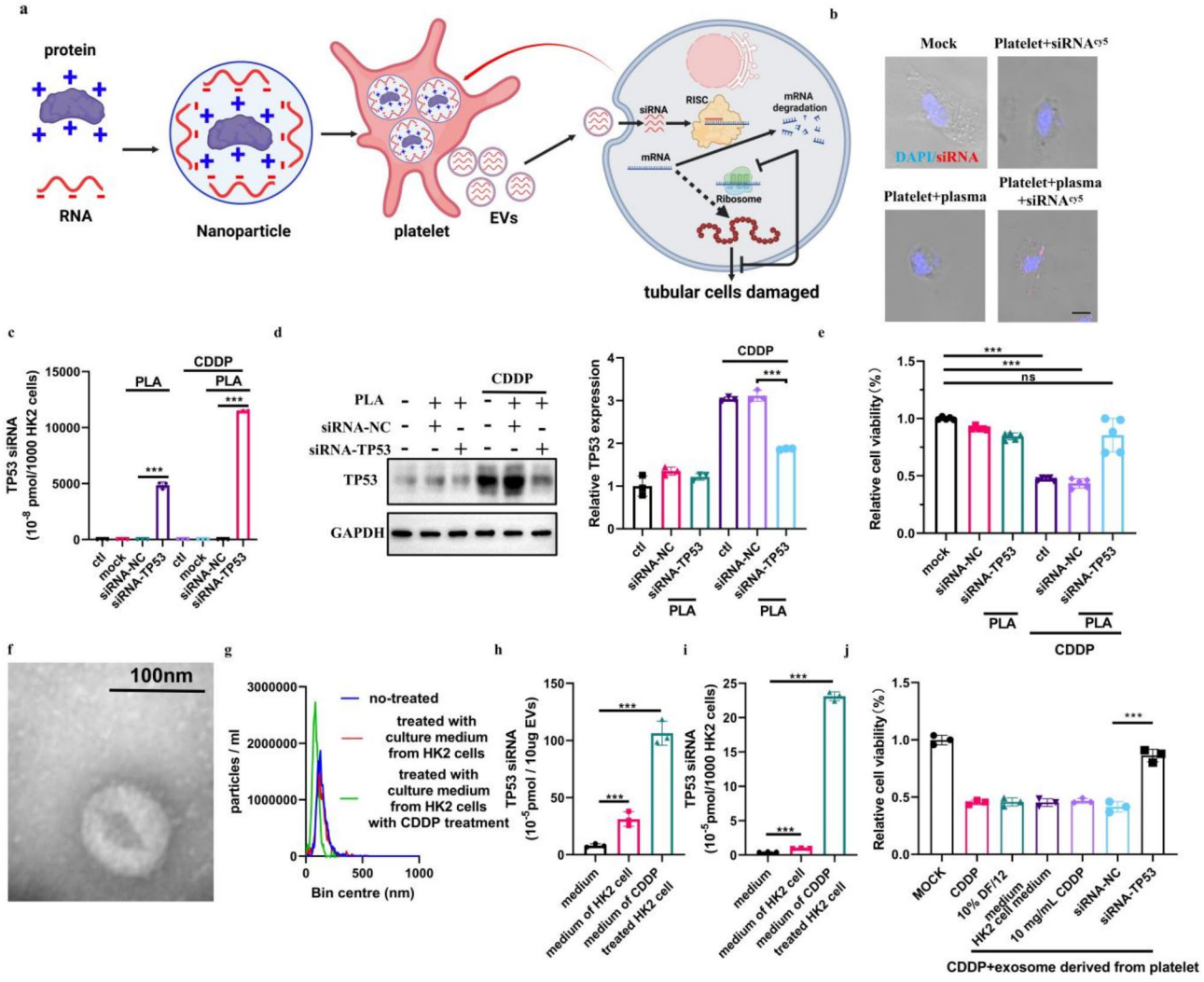

Fig. 3 Platelets deliver TP53 siRNA to renal tubular cells and protect them from CDDP-induced toxicity. (**a**) Platelets deliver TP53 siRNA to tubule cells to reduce TP53 levels and protect them from CDDP-induced toxicity via EVs. (**b**) Images of HK-2 cells incubated with platelets. Blue: cell nuclear staining by PI; red: Cy5-labeled TP53 siRNA. Scale bar: 20 μm. (**c**) TP53 siRNA levels in HK-2 cells incubated with platelets. HK-2 cells were treated with or without CDDP. (**d**) TP53 protein levels in HK-2 cells incubated with platelets. HK-2 cells were treated with or without CDDP. (**e**) Viability of HK-2 cells treated with or without CDDP. (**f**) TEM image of EVs isolated from platelets. Scale bar: 100 nm. (**g**) NTA analysis of EVs isolated from platelets treated with control medium, HK-2 cell culture medium or CDDP-treated HK-2 cell culture medium. Platelets not treated with cell culture medium (untreated) served as controls. (**h**) TP53 siRNA levels in EVs isolated from platelets treated with control medium, HK-2 cell culture medium or CDDP-treated HK-2 cell culture medium. (**i**) TP53 siRNA levels in HK-2 cells incubated with EVs isolated from platelets treated with control medium, HK-2 cell culture medium or CDDP-treated HK-2 cell culture medium. (**j**) Viability of HK-2 cells incubated with EVs isolated from platelets treated with control medium, HK-2 cell culture medium or CDDP-treated HK-2 cell culture medium. Each experiment was repeated three times. Statistical differences between groups were assessed by independent-samples t tests. Data with a P value < 0.05 were considered statistically significant. The plasma and platelets were isolated from human blood

which play key roles in wound healing, cell activation and proliferation, angiogenesis, immune cell recruitment, inflammation, bone regeneration, and cartilage repair [39]. Platelet-derived EVs account for approximately 70% of total plasma EVs and have been shown to facilitate intercellular communication by transferring nucleic acids, proteins, and organelles [40]. To investigate whether platelets can transfer TP53 siRNA into tubular cells via platelet-derived EVs, platelet-derived EVs were isolated via ultrahigh-speed centrifugation as previously described [33, 40]. The isolated platelet-derived EVs were characterized by TEM, NTA, and western blotting (Fig. 3f-g and Figure S4). Notably, the concentration of EVs released from platelets significantly increased when platelets were incubated with EV-free medium from CDDP-treated HK-2 cells (Fig. 3g and Figure S5a). These findings suggest that CDDP-stimulated HK-2 cells could increase platelet EV secretion. As shown in Fig. 3h, platelet-derived EVs were enriched with siRNAs, and the siRNA content in platelet-derived EVs was

much greater when platelets were incubated with EV-free medium from CDDP-treated HK-2 cells. Furthermore, TP53 siRNA was successfully delivered into HK-2 cells via platelet-derived EVs, protecting them from CDDP-induced cell death (Fig. 3i-j).

To verify that TP53 siRNA is delivered into renal tubular cells via platelet-derived EVs, we treated platelets with GW4869, a neutral sphingomyelinase inhibitor commonly used to block EV generation. GW4869 significantly inhibited EV release from platelets (Figure S5b). Platelets were then incubated with nanoparticles formed by TP53 siRNA in the presence of plasma. GW4869 did not affect nanoparticle uptake by platelets (Figure S5c). However, when platelets loaded with TP53 siRNA were cocultured with HK-2 cells, GW4869 blocked the delivery of TP53 siRNA from platelets to HK-2 cells via EVs (Figure S5d). This inhibition prevented TP53 protein suppression (Figure S5e) and attenuated the protective effect against CDDP-induced cell death (Figure S5f).

To further confirm that the protective effect on renal tubular cells is specifically mediated by TP53 siRNA delivered via platelet-derived EVs rather than other components in platelet-derived EVs, we first transfected HK-2 cells with a TP53 siRNA inhibitor (TP53 siRNA antisense) that specifically binds to TP53 siRNA (Figure S6a). These cells were then incubated with EVs released from TP53 siRNA-loaded platelets. Compared with HK-2 cells directly incubated with platelet-derived EVs, those pretransfected with the TP53 siRNA inhibitor presented no upregulation of TP53 siRNA (Figure S6b), no suppression of the TP53 protein (Figure S6c-d), and no protection against CDDP-induced cell death (Figure S6e). These findings indicate that the protective effect is specifically mediated by TP53 siRNA delivered via platelet-derived EVs.

The biodistribution of siRNAs delivered by platelets in vivo.

Platelets are the first cells to arrive at sites of acute injury during AKI, where they rapidly release a diverse array of bioactive mediators that play crucial roles in modulating inflammation and hemostasis [41]. Consequently, strategies involving the manipulation of platelet-derived factors or the use of platelet-rich products, such as platelet-rich plasma or platelet-derived EVs, hold promise for facilitating renal regeneration and improving clinical outcomes in patients with acute kidney injury [15–17, 41–45]. The objective of this study was to investigate whether platelets could self-target damaged kidneys and deliver Trp53 siRNA into injured tubular cells. Thus, 24 h after AKI was induced via bilateral renal ligation (IRI model) or intraperitoneal injection of cisplatin (CDDP model), the mice were injected with synthetic Cy5-labeled siRNA-loaded platelets (1 × 107 platelets per mouse) via the tail vein. The control group received a direct tail vein injection of synthetic Cy5-labeled siRNA. The mice were anesthetized and perfused via the heart after six hours, and tissues (brain, heart, lung, liver, kidney, and spleen) were collected and analyzed for fluorescence signal intensity. The results showed that directly injected Cy5-labeled Trp53 siRNA accumulated predominantly in the liver. In contrast, siRNAs delivered by platelets aggregated specifically in kidneys damaged by IRI or CDDP (Fig. 4a-b). Notably, platelet-encapsulated siRNA did not enter tissues in normal mice, likely because platelets do not actively infiltrate healthy tissues and remain in circulation until clearance (Fig. 4a-b). Further analysis by immunofluorescence revealed that platelet-delivered Cy5-labeled siRNA accumulated in damaged renal tubular cells, as indicated by colocalization with Mcp1, the activation marker of damaged tubular cells in acute kidney injury [46] (Fig. 4c and Figure S7).

Autologous delivery of Trp53 SiRNA to platelets for the treatment of acute kidney injury

To further evaluate the biodistribution of autologous platelet delivery of self-assembling nanoparticles composed of autologous plasma proteins and Trp53 siRNA in AKI mice, AKI mice induced by IRI or CDDP were injected with platelets or synthetic siRNA via the tail vein, with AKI induction occurring 48 h later. Each mouse received 1 × 107 platelets every two days for a total of four injections. Two days after the final injection, urine was collected, and the mice were euthanized to harvest the brain, heart, lung, liver, kidney, and spleen for Western blotting and immunohistochemical staining to assess therapeutic efficacy (Fig. 5a). The concentration of Trp53 siRNA in the tissues was measured via RT–qPCR. Trp53 siRNA delivered by platelets was predominantly localized in the kidneys (Fig. 5b). In contrast, synthetic Cy5-labeled Trp53 siRNA injected directly via the tail vein was almost undetectable (Fig. 5b). Trp53 mRNA and protein levels were assessed via RT–qPCR, Western blotting, and immunohistochemistry. RT–qPCR revealed significant upregulation of Trp53 mRNA in the kidneys of mice with IRI- or CDDP-induced AKI (Figure S8a), which was markedly reduced in mice treated with Trp53 siRNA-loaded platelets (Figure S8a). Trp53 mRNA levels in other tissues (brain, heart, lung, liver, and spleen) remained unchanged (Figure S8a). Western blot analysis revealed a significant increase in Trp53 protein expression in the kidneys of AKI mice, which was significantly attenuated by Trp53 siRNA-loaded platelet treatment (Fig. 5c and Figure S8b). The results of immunohistochemical staining for the Trp53 protein were consistent with these findings (Figure S8c-d).

The therapeutic potential of autologous platelet delivery of self-assembling nanoparticles composed of autologous plasma proteins and Trp53 siRNA was evaluated

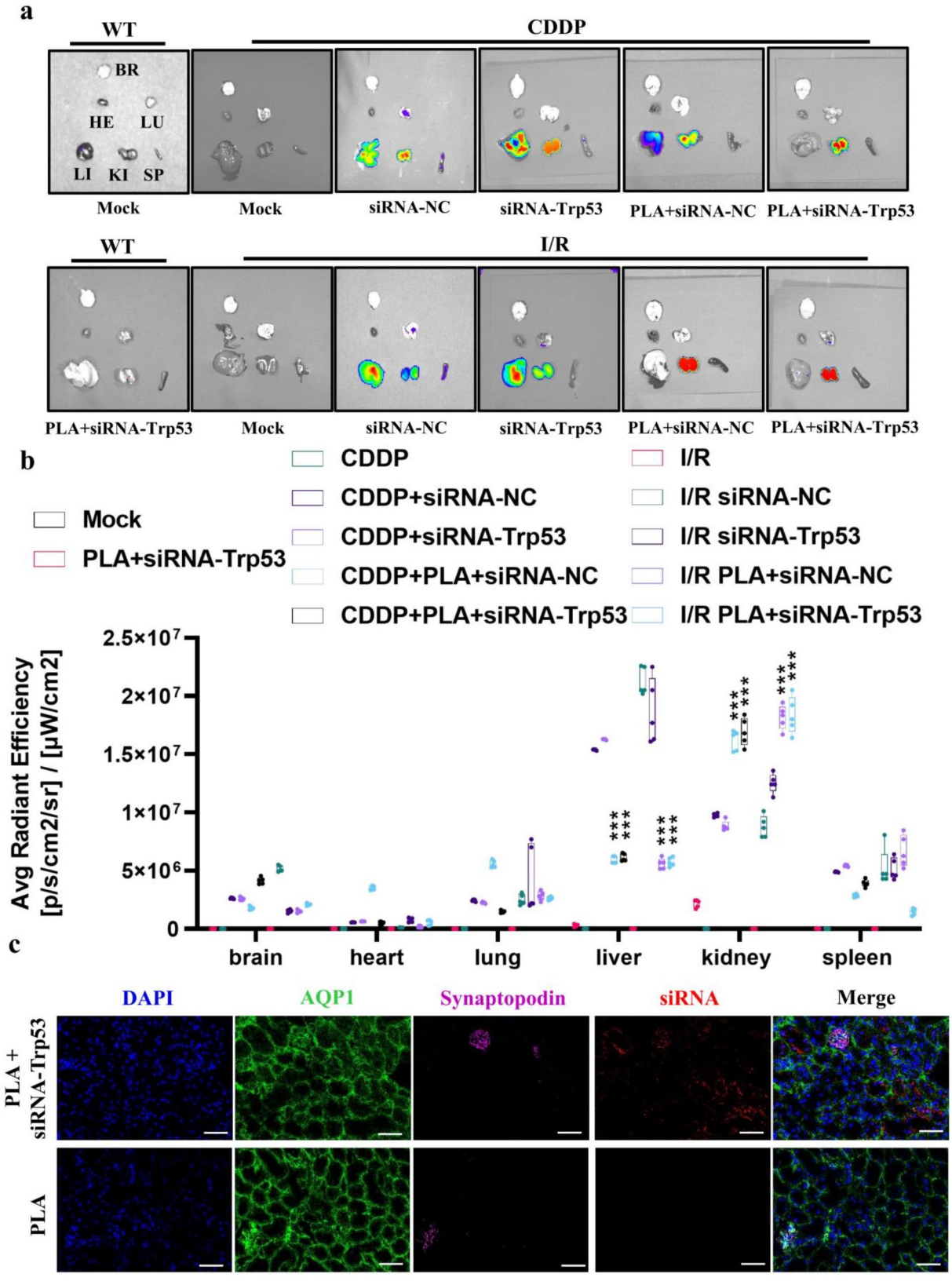

Fig. 4 Platelets primarily self-target tubule cells in AKI model mice induced by IRI and CDDP. (**a**-**b**) Fluorescence of Cy5-siRNA delivered by platelets through tail vein injection in AKI model mice induced by IRI and CDDP. a: Representative image; b: Fluorescence intensity of Cy5-siRNA. (**c**) Fluorescence image of Cy5-siRNA in a kidney section. DAPI: nucleus; AQP1: renal tubular cells; Synaptopodin: glomerulus. Scale bar: 50 μm

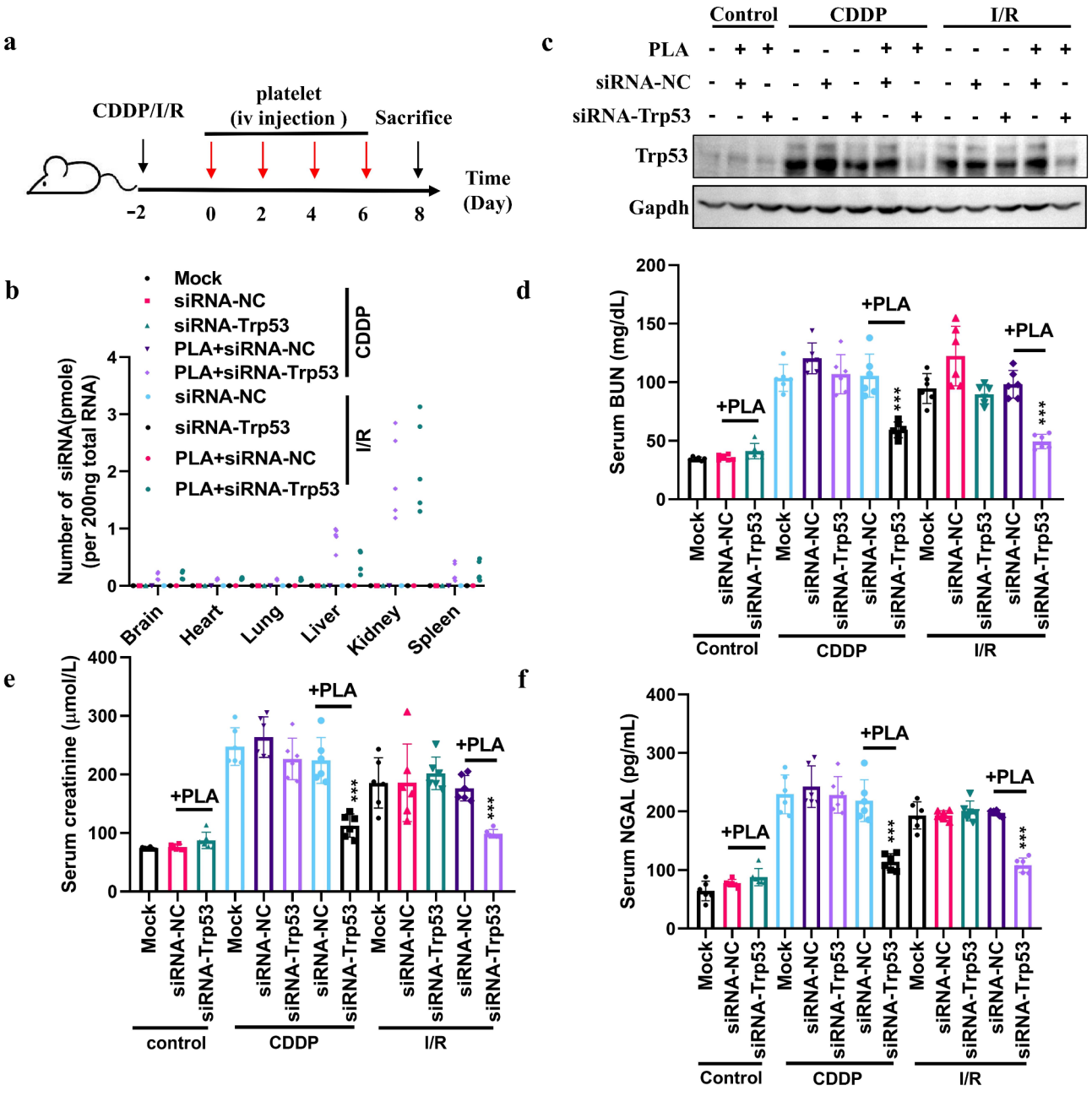

Fig. 5 Platelet treatment modulates tubular cells following IRI and CDDP-induced AKI. (**a**) Experimental scheme of intravital imaging and Trp53 siRNA delivery. (**b**) Trp53 siRNA levels in the tissues of AKI model mice induced by IRI and CDDP and healthy control mice (mock). (**c**) Trp53 protein levels in the kidneys of AKI model mice induced by IRI and CDDP and healthy control mice injected with siRNA-NC-, siRNA-Trp53-, or siRNA-NC-loaded platelets or siRNA-Trp53-loaded platelets through the tail vein. (**d**-**f**) Serum BUN, creatinine and NGAL levels in the kidneys of AKI model mice induced by IRI and CDDP and healthy control mice injected with siRNA-NC, siRNA-Trp53, siRNA-NC-loaded platelets or siRNA-Trp53-loaded platelets through the tail vein. Statistical differences between groups were assessed by independent-samples t tests. Data with a P value < 0.05 were considered statistically significant

via acute renal injury markers, including blood urea nitrogen (BUN), serum creatinine (sCr), and neutrophil gelatinase-associated lipocalin (NGAL). Immunohistochemistry and histopathological assessments (including hematoxylin and eosin (H&E) staining for pathological scoring and analysis of Trp53 downstream proteins such as B-cell lymphoma protein 2 (Bcl-2), Bcl-2-associated X (Bax), and cleaved caspase 3) were also performed. Additionally, the terminal deoxynucleotidyl transferase (TdT) dUTP nick-end labeling (TUNEL) assay was used to detect apoptotic cells. Consistent with previous reports [34], BUN, sCr and NGAL levels were significantly elevated in mice with AKI induced by IRI or CDDP compared with those in controls (Fig. 5d-f). However, these

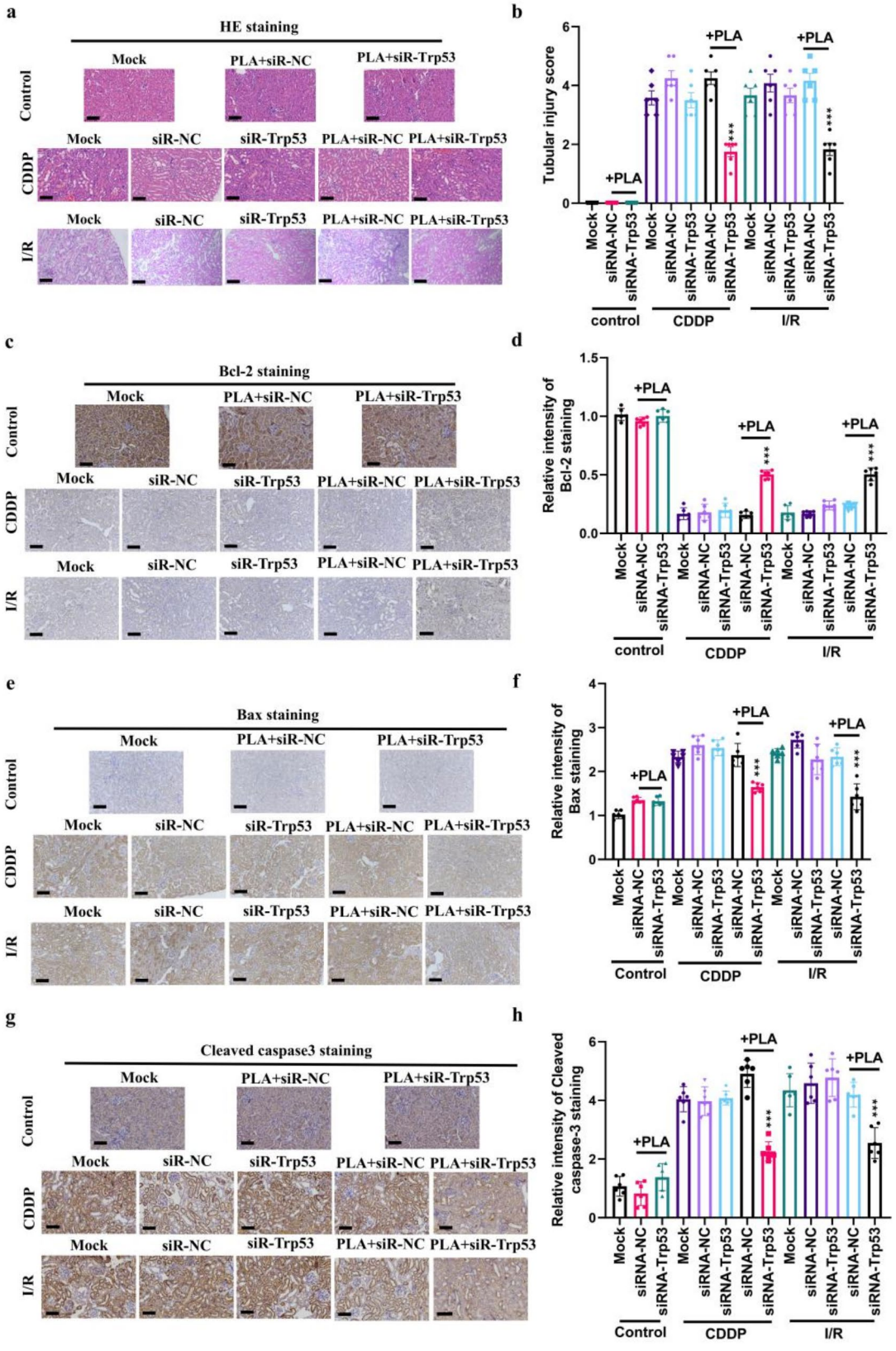

Fig. 6 (See legend on next page.)

(See figure on previous page.)

Fig. 6 Histological evaluation of IRI- and CDDP-induced AKI mice treated with platelets. (**a**-**b**) The tubular injury scores of AKI model mice induced by IRI and CDDP and healthy control mice injected with siRNA-NC, siRNA-Trp53, or siRNA-NC-loaded platelets or siRNA-Trp53-loaded platelets through the tail vein were determined via H&E staining. (**c**-**h**) Bcl-2, Bax and cleaved caspase-3 levels in the kidneys of AKI model mice induced by IRI and CDDP and healthy control mice injected with siRNA-NC, siRNA-Trp53, or siRNA-NC-loaded platelets or with siRNA-Trp53-loaded platelets through the tail vein or left untreated by immunohistochemistry (six mice in each group). Statistical differences between groups were assessed by independent-samples t tests. Data with a P value < 0.05 were considered statistically significant. Scale bar: 50 μm

indicators returned to normal levels in AKI mice treated with Trp53 siRNA-loaded platelets (Fig. 5d-f). Histological evaluation via H&E staining revealed increased tubular injury scores in AKI mice induced by IRI or CDDP. In contrast, the tubular injury score was significantly reduced in AKI mice treated with Trp53 siRNA-loaded platelets (Fig. 6a-b and Figure S9). Immunohistochemical analysis revealed that the expression of Bcl-2, an anti-apoptotic protein downstream of Trp53, was significantly decreased in AKI model mice induced by IRI or CDDP (Fig. 6c-d and Figure S10). Conversely, Bcl-2 was upregulated in AKI mice treated with Trp53 siRNA-loaded platelets (Fig. 6c-d and Figure S10). Conversely, the levels of Bax and cleaved caspase 3, proapoptotic proteins downstream of Trp53, were significantly increased in AKI model mice induced by IRI or CDDP (Fig. 6e-h and Figure S11-S12). However, these proteins were downregulated in AKI mice treated with Trp53 siRNA-loaded platelets (Fig. 6e-h and Figure S11-S12). The TUNEL assay, which detects apoptotic cells undergoing extensive DNA degradation, also demonstrated a similar trend (Figure S13). The mRNA levels of Cxcl2, IL-1β, and Ccl2 were also examined in both IRI- and CDDP-induced AKI model mice. As shown in Figure S14, these mRNA levels were significantly elevated in AKI mice subjected to IRI or CDDP, as shown in previous studies [1]. In contrast, AKI mice treated with Trp53 siRNA-loaded platelets presented markedly reduced mRNA levels of Cxcl2, IL-1β, and Ccl2 (Figure S14).

To assess the hepatotoxicity and cardiotoxicity associated with platelet-mediated siRNA delivery, histological analyses of the liver and heart were conducted via H&E staining. Extensive evidence has shown that intravenous injection of naked siRNAs can lead to liver and heart injury due to their accumulation in the liver and subsequent activation of pattern recognition receptor-induced inflammatory pathways [47–51]. This issue poses a significant barrier to the widespread clinical application of siRNA-based therapies. Histological evaluation via H&E staining revealed that the overall structure, integrity, and immune infiltration levels of the liver and heart were nearly identical to those of healthy controls when siRNAs were delivered by platelets (Figure S15). Moreover, serum alanine aminotransferase (ALT) levels were significantly elevated in mice following direct injection of siRNAs (Figure S16a). However, the platelet-delivered siRNAs did not aggregate in the liver; instead, they accumulated in the damaged kidneys without causing an increase in the serum ALT level (Fig. 4a-b and Figure S16a). Additionally, chemokines such as Cxcl2, IL-1β, and Ccl2, which are involved in the inflammatory pathways triggered by siRNA injection, were significantly upregulated in the liver following direct siRNA injection. In contrast, these chemokines remained unchanged in the liver when siRNAs were delivered by platelets (Figure S16b-d).

Discussion

Despite significant advances in our understanding of the pathophysiology of AKI, there remains a critical gap in effective and safe therapeutic options for treating ischemic AKI [1]. Consequently, mortality and morbidity rates remain high. The pathogenesis of AKI is multifaceted and involves mechanisms such as renal tubular cell apoptosis and necrosis, oxidative stress, and vascular injury [1]. The tumor suppressor p53 is a key factor in AKI pathogenesis and renal repair following injury [1, 52], and inhibiting p53 in renal tubular cells has emerged as a promising strategy for treating AKI [21–25, 27–29]. Molitoris et al. demonstrated that p53 inhibition in renal tubules via siRNA could prevent apoptosis and renal impairment in AKI models induced by ischemia−reperfusion injury (IRI) and cisplatin [27]. However, the effective dose in mice is as high as 12 mg/kg [27], rendering the treatment prohibitively expensive and increasing the risk of inflammation and side effects due to high siRNA concentrations. To address these issues, researchers have attempted to treat AKI with lower siRNA doses (e.g., 0.1 mg/kg or 0.5 mg/kg) [21, 22]. Unfortunately, these reduced doses are ineffective at treating AKI [21, 23, 24, 26]. Consistent with these findings, our study revealed that a dose of 0.1 mg/kg Trp53 siRNA, which was significantly greater than that delivered by platelets, failed to produce therapeutic effects in mouse models of AKI. While siRNAs hold potential as therapeutic agents, their use is limited by several challenges, including degradation, inefficient delivery, and off-target effects. Hydrodynamic injection of large doses of free siRNA is effective in mice but is not feasible in humans because of safety concerns [47, 53, 54]. To overcome these limitations, siRNAs must be encapsulated in a delivery system. Several studies have confirmed that siRNAs can be encapsulated in synthetic polymeric nanomaterials or natural EVs for in vivo delivery [47, 53, 54]. However, these methods involve either the use of synthetic nanomaterials with

potential side effects or the costly production of natural EVs by cells [47, 53, 54].

Previous studies have shown that RNA nanoparticles can be formed by mixing RNAs with positively charged proteins or peptides [31, 55]. These cationic proteins or peptides can serve as carriers for siRNA-based therapeutics. Our study demonstrated that plasma cationic proteins can spontaneously form nanoparticles with siRNA, as previously reported [31]. These nanoparticles can be utilized in siRNA drug therapy by combining a patient's plasma proteins with siRNA to create delivery-capable nanoparticles. This approach eliminates the need for synthetic polymer nanomaterials or costly in vitro culture, representing an advancement in siRNA drug delivery. However, there are limitations to this method. The siRNA nanoparticles formed by mixing plasma proteins with siRNA lack inherent targeting capabilities. Modifying plasma proteins or siRNAs to achieve targeted delivery remains challenging. To address this limitation, we leveraged platelets, the most abundant nucleated cells in the body, which possess an intrinsic targeting function. By incorporating platelets, we achieved targeted delivery of siRNA nanoparticles generated from the patient's own plasma proteins and siRNA. This strategy effectively overcomes the lack of targeting in siRNA nanoparticles while maintaining the benefits of using autologous materials.

Platelets are highly sensitive to environmental changes and circulate in significant numbers (150–400 billion cells per liter of blood in humans), enabling a rapid response to biological perturbations from injury or infection [41]. They continuously monitor their surroundings via a plethora of cell surface receptors and adhesion molecules. During AKI, platelets aggregate at sites of renal injury, where they orchestrate AKI regulation by secreting proteins, EVs, and other bioactive substances [41]. Previous studies have extensively leveraged this mechanism to explore the delivery of drugs for treating AKI via platelets or nanoparticles formed by platelet membranes [15, 42–44, 56]. In this study, we leveraged the inherent targeting of platelets to injury sites to exploit autologous platelets to encapsulate nanoparticles containing p53 siRNA. These platelets autonomously navigate to the renal injury site, where they are regulated by signaling molecules to release numerous EVs. These EVs fuse with injured tubular cells to transfer p53 siRNA and inhibit p53 expression, thereby preventing tubular cell apoptosis and treating AKI. The utilization of autologous plasma proteins for siRNA encapsulation ensures in vivo delivery by autologous platelets. This approach is superior to conventional methods that utilize lipid nanoparticles (LNPs) or EVs for siRNA delivery, as it avoids the use of exogenous materials. It minimizes the use of chemically synthesized substances, as siRNAs are enveloped by proteins, platelets, and EVs throughout, reducing an organism's exposure to foreign substances and the potential for side effects. Moreover, the use of autologous proteins and platelets for nucleic acid drug delivery could pave the way for bedside nucleic acid drug delivery systems. This approach may eliminate the need for cryopreservation required for lipid nanoparticle or extracellular vesicle delivery, reduce the material costs associated with siRNA drugs, and facilitate large-scale clinical applications of siRNA therapies. Building on our developed method, we conceptualized a bedside nucleic acid drug delivery system tailored for acute kidney injury (Figure S17). In future research, we will conduct further feasibility studies to validate this approach.

This study has several limitations that warrant acknowledgment. First, although we identified plasma cationic proteins that self-assemble with siRNA to form nanoparticles through protein mass spectrometry, we could not pinpoint the specific cationic protein that plays the most central role in nanoparticle formation. Identifying this core cationic protein could enable direct nanoparticle formation with siRNA for drug delivery, making the process more controllable and scalable. Second, we did not investigate whether there is selectivity in the encapsulation of siRNA by platelets into platelet-derived EVs. Previous studies have shown that cells selectively encapsulate certain nucleic acids with specific sequences or modifications into EVs [57, 58]. These findings suggest that similar selectivity may exist for platelet-encapsulated siRNA. Therefore, when designing siRNAs, it may be necessary to incorporate specific sequences or modifications to increase the encapsulation efficiency. An incorrect design could result in the encapsulation of siRNAs into platelet-derived EVs, thereby reducing therapeutic efficacy. Conversely, optimizing the siRNA design could improve the encapsulation efficiency, potentially lowering the required siRNA dosage and enhancing therapeutic outcomes. Third, our study confirmed only in vitro that inhibiting platelet-derived EV release can block siRNA delivery to renal tubular cells. We lack in vivo evidence. In future work, we aim to use gene editing techniques to completely inhibit platelet EV release and observe whether siRNA delivery to damaged renal tubular cells is still possible in vivo. Fourth, while we demonstrated that the culture medium of damaged renal tubular cells promotes platelet EV release, the underlying mechanism remains unclear. Future research will focus on elucidating the molecular pathways by which damaged renal tubular cells increase platelet EV release, both in vitro and in vivo, to better understand the interaction between renal tubular cells and platelets in acute kidney injury (AKI). Fifth, our investigation of the distribution of platelet-derived siRNAs in mice relied on fluorescence imaging, confocal microscopy, and quantitative PCR.

However, the Cy5 wavelength limits our ability to obtain in vivo fluorescence images. We plan to employ advanced techniques, such as two-photon imaging, in future studies to observe platelet-delivered siRNA dynamics and distribution more accurately in animal models. Finally, our study primarily used cell and mouse models to assess the therapeutic effects of platelet-delivered siRNA in AKI. We lacked large mammalian models and clinical trials. Moving forward, we aim to validate the therapeutic efficacy of platelet-delivered siRNA in larger mammalian models and, ultimately, in clinical settings to lay the groundwork for its application in treating AKI.

In conclusion, our study demonstrated that synthetic siRNAs can rapidly form nanoparticles in plasma and be autonomously taken up by platelets. These platelet-loaded siRNAs exhibit self-targeting properties, enabling their selective delivery to kidneys affected by AKI and subsequent uptake by renal tubular cells via extracellular vesicles. This process effectively reduces target protein levels and alleviates renal injury. Thus, the use of platelets as a delivery vehicle for siRNA represents a promising therapeutic approach for AKI, offering a direct intracellular delivery method for siRNAs to target cells and providing a valuable strategy for AKI management. Moreover, platelets can self-target other damaged tissues, such as the liver, lungs, and tumors [59]. Therefore, the platelet self-targeting strategy for drug delivery demonstrated in this study could be applied to other diseases beyond AKI. However, further studies using a broader range of disease models are needed to confirm the efficacy of this approach in conditions other than AKI.

Supplementary Information

The online version contains supplementary material available at https://doi.org/10.1186/s12951-025-03338-6.

Supplementary Material 1

Supplementary Material 2

Supplementary Material 3

Author contributions

HL, KZ, YY and CQ designed the experiments. JW, HH, SC, FW, MJ, GH, CW, KL, XZ and ZH performed the experiments and analyzed the results. HL and KZ wrote the manuscript.

Funding

This work was supported by grants from the National Natural Science Foundation of China (No. 31801088, No. 32170783).

Data availability

No datasets were generated or analysed during the current study.

Declarations

Ethical approval

The studies involving animal experiments were reviewed and approved by the Ethics Committee of China Pharmaceutical University.

Declaration of AI-assisted technologies in the writing process

During the preparation of this work, the authors used ChatGPT only for improving language and readability. After using this tool, the authors reviewed and edited the content as needed and take full responsibility for the content of the publication.

Competing interests

The authors declare no competing interests.

Received: 5 October 2024 / Accepted: 17 March 2025
Published online: 29 March 2025

References

1. Kellum JA, Romagnani P, Ashuntantang G, Ronco C, Zarbock A, Anders HJ. Acute kidney injury. Nat Rev Dis Primers. 2021;7:52.
2. Tang CY, Livingston MJ, Safirstein R, Dong Z. Cisplatin nephrotoxicity: new insights and therapeutic implications. Nat Rev Nephrol. 2023;19:53–72.
3. Tang Q, Khvorova A. RNAi-based drug design: considerations and future directions. Nat Rev Drug Discov. 2024;23:341–64.
4. Schagen FHE, Ossevoort M, Toes REM, Hoeben RC. Immune responses against adenoviral vectors and their transgene products: a review of strategies for evasion. Crit Rev Oncol Hematol. 2004;50:51–70.
5. Davis ME, Zuckerman JE, Choi CH, Seligson D, Tolcher A, Alabi CA, Yen Y, Heidel JD, Ribas A. Evidence of RNAi in humans from systemically administered SiRNA via targeted nanoparticles. Nature. 2010;464:1067–70.
6. Zhou YL, Yang QQ, Yan YY, Zhang L, Wang QH, Ju F, Tang JB. Gene-Loaded Nanoparticle-Coated sutures provide effective gene delivery to enhance tendon healing. Mol Ther. 2019;27:1534–46.
7. Yang QQ, Zhang LZ, Zhou YL, Tang JB. Morphological changes of macrophages and their potential contribution to tendon healing. Colloids Surf B-Biointerfaces. 2022;209.
8. Hou MY, Wei YS, Zhao ZY, Han WQ, Zhou RX, Zhou Y, Zheng YR, Yin LC. Immuno-Engineered nanodecoys for the Multi-Target Anti-Inflammatory treatment of autoimmune diseases. Adv Mater. 2022;34.
9. Wang TY, Zhou TT, Xu MM, Wang S, Wu AQ, Zhang MY, Zhou YL, Shi JH. Platelet membrane-camouflaged nanoparticles carry MicroRNA inhibitor against myocardial ischaemia-reperfusion injury. J Nanobiotechnol. 2022;20.
10. Feltrin FD, Agner T, Sayer C, Lona LMF. Curcumin encapsulation in functional PLGA nanoparticles: A promising strategy for cancer therapies. Adv Colloid Interface Sci. 2022;300.
11. Choi B, Park W, Park SB, Rhim WK, Han DK. Recent trends in cell membrane-cloaked nanoparticles for therapeutic applications. Methods. 2020;177:2–14.
12. Fang MK, Liu R, Fang YL, Zhang DG, Kong B. Emerging platelet-based drug delivery systems. Biomed Pharmacother. 2024;177.
13. Sender R, Fuchs S, Milo R. Revised estimates for the number of human and bacteria cells in the body. PLoS Biol. 2016;14:e1002533.
14. Carney EF. Acute kidney injury: role of platelet activation and NETs in renal IRI. Nat Rev Nephrol. 2016;12:715.
15. Yang J, Chen C, Miao X, Wang T, Guan Y, Zhang L, Chen S, Zhang Z, Xia Z, Kang J, et al. Injury site specific Xenon delivered by platelet Membrane-Mimicking hybrid microbubbles to protect against acute kidney injury via Inhibition of cellular senescence. Adv Healthc Mater. 2023;12:e2203359.
16. Yang J, Miao X, Guan Y, Chen C, Chen S, Zhang X, Xiao X, Zhang Z, Xia Z, Yin T, et al. Microbubble functionalization with platelet membrane enables targeting and early detection of Sepsis-Induced acute kidney injury. Adv Healthc Mater. 2021;10:e2101628.
17. Okubo K, Kurosawa M, Kamiya M, Urano Y, Suzuki A, Yamamoto K, Hase K, Homma K, Sasaki J, Miyauchi H, et al. Macrophage extracellular trap formation promoted by platelet activation is a key mediator of rhabdomyolysis-induced acute kidney injury. Nat Med. 2018;24:232–8.
18. Gu XR, Tai YF, Liu Z, Zhang XY, Liu K, Zhou LY, Yin WJ, Deng YX, Kong DL, Midgley AC, Zuo XC. Layer-by-Layer assembly of Renal-Targeted polymeric nanoparticles for robust Arginase-2 knockdown and Contrast-Induced acute kidney injury prevention. Adv Healthc Mater. 2024.
19. Xie DP, Wang J, Hu GZ, Chen CL, Yang H, Ritter JK, Qu Y, Li NJ. Kidney-Targeted delivery of Prolyl hydroxylase domain protein 2 small interfering RNA with nanoparticles alleviated renal ischemia/reperfusion injury. J Pharmacol Exp Ther. 2021;378:235–43.

20. Liu L, Li Y, Hu Z, Su J, Huo Y, Tan B, Wang X, Liu Y. Small interfering RNA targeting Toll-like receptor 9 protects mice against polymicrobial septic acute kidney injury. Nephron Exp Nephrol. 2012;122:51–61.
21. Alidori S, Akhavein N, Thorek DLJ, Behling K, Romin Y, Queen D, Beattie BJ, Manova-Todorova K, Bergkvist M, Scheinberg DA, McDevitt MR. Targeted fibrillar nanocarbon RNAi treatment of acute kidney injury. Sci Transl Med. 2016;8.
22. Tang WM, Chen Y, Jang HS, Hang Y, Jogdeo CM, Li J, Ding L, Zhang CH, Yu A, Yu F, et al. Preferential SiRNA delivery to injured kidneys for combination treatment of acute kidney injury. J Controlled Release. 2022;341:300–13.
23. Li CX, Zhao WZ, Hu ZJ, Yu HX. Cholesterol-Modified DNA Nanostructures Serve as Effective Non-Viral Carriers for Delivering siRNA to the Kidneys to Prevent Acute Kidney Injury. Small. 2024.
24. Tang WM, Panja S, Jogdeo CM, Tang SY, Ding L, Yu A, Foster KW, Dsouza D, Chhonker YS, Jensen-Smith H et al. Modified Chitosan for effective renal delivery of SiRNA to treat acute kidney injury. Biomaterials 2022;285.
25. Thielmann M, Corteville D, Szabo G, Swaminathan M, Lamy A, Lehner LJ, Brown CD, Noiseux N, Atta MG, Squiers EC, et al. Teprasiran, a small interfering RNA, for the prevention of acute kidney injury in High-Risk patients undergoing cardiac surgery A randomized clinical study. Circulation. 2021;144:1133–44.
26. Tang TT, Wang B, Li ZL, Wen Y, Feng ST, Wu M, Liu D, Cao JY, Yin Q, Yin D, et al. Kim-1 targeted extracellular vesicles: A new therapeutic platform for RNAi to treat AKI. J Am Soc Nephrol. 2021;32:2467–83.
27. Molitoris BA, Dagher PC, Sandoval RM, Campos SB, Ashush H, Fridman E, Brafman A, Faerman A, Atkinson SJ, Thompson JD, et al. SiRNA targeted to p53 attenuates ischemic and cisplatin-induced acute kidney injury. J Am Soc Nephrol. 2009;20:1754–64.
28. Fu SS, Hu XR, Ma ZW, Wei QQ, Xiang XH, Li SY, Wen L, Liang YM, Dong Z. p53 in proximal tubules mediates chronic kidney problems after cisplatin treatment. Cells. 2022;11.
29. Kelly KJ, Plotkin Z, Vulgamott SL, Dagher PC. P53 mediates the apoptotic response to GTP depletion after renal ischemia-reperfusion: protective role of a p53 inhibitor. J Am Soc Nephrol. 2003;14:128–38.
30. Inaba S, Nagahara S, Makita N, Tarumi Y, Ishimoto T, Matsuo S, Kadomatsu K, Takei Y. Atelocollagen-mediated systemic delivery prevents immunostimulatory adverse effects of SiRNA in mammals. Mol Ther. 2012;20:356–66.
31. Liu J, Li W, Li J, Song E, Liang H, Rong W, Jiang X, Xu N, Wang W, Qu S, et al. A novel pathway of functional MicroRNA uptake and mitochondria delivery. Adv Sci (Weinh). 2023;10:e2300452.
32. Yang R, Zhang H, Chen S, Lou K, Zhou M, Zhang M, Lu R, Zheng C, Li L, Chen Q, et al. Quantification of urinary podocyte-derived migrasomes for the diagnosis of kidney disease. J Extracell Vesicles. 2024;13:e12460.
33. Liang H, Yan X, Pan Y, Wang Y, Wang N, Li L, Liu Y, Chen X, Zhang CY, Gu H, Zen K. MicroRNA-223 delivered by platelet-derived microvesicles promotes lung cancer cell invasion via targeting tumor suppressor EPB41L3. Mol Cancer. 2015;14:58.
34. Fu Y, Tang CY, Cai J, Chen GC, Zhang DS, Dong Z. Rodent models of AKI-CKD transition. Am J Physiology-Renal Physiol. 2018;315:F1098–106.
35. Copolovici DM, Langel K, Eriste E, Langel U. Cell-penetrating peptides: design, synthesis, and applications. ACS Nano. 2014;8:1972–94.
36. Wang H, Wang Z, Chen W, Wang W, Shi W, Chen J, Hang Y, Song J, Xiao X, Dai Z. Self-assembly of photosensitive and radiotherapeutic peptide for combined photodynamic-radio cancer therapy with intracellular delivery of miRNA-139-5p. Bioorg Med Chem. 2021;44:116305.
37. Chen B, Khodadoust MS, Liu CL, Newman AM, Alizadeh AA. Profiling tumor infiltrating immune cells with CIBERSORT. Methods Mol Biol. 2018;1711:243–59.
38. Liu J, Li W, Li J, Song E, Liang H, Rong W, Jiang X, Xu N, Wang W, Qu S et al. A novel pathway of functional microRNA uptake and mitochondria delivery. bioRxiv. 2022.
39. Spakova T, Janockova J, Rosocha J. Characterization and therapeutic use of extracellular vesicles derived from platelets. Int J Mol Sci. 2021;22.
40. Muttiah B, Ng SL, Lokanathan Y, Ng MH, Law JX. Beyond blood clotting: the many roles of Platelet-Derived extracellular vesicles. Biomedicines. 2024;12.
41. Jansen MPB, Florquin S, Roelofs J. The role of platelets in acute kidney injury. Nat Rev Nephrol. 2018;14:457–71.
42. Zhang M, Li Y, Xu T, Liu B, Liu Y, Cheng X, Pan J, Wang J. A rapamycin-loading platelet membrane hybrid liposome with anti-inflammation effect and long-lasting repair capability for acute kidney injury. J Control Release. 2025;380:927–42.
43. Yao S, Wu D, Hu X, Chen Y, Fan W, Mou X, Cai Y, Yang X. Platelet membrane-coated bio-nanoparticles of indocyanine Green/elamipretide for NIR diagnosis and antioxidant therapy in acute kidney injury. Acta Biomater. 2024;173:482–94.
44. Ji C, Zhang J, Zhou Z, Shi H, Liu W, Sun F, Zhang C, Zhang L, Sun Z, Qian H. Platelet-rich plasma promotes MSCs exosomes paracrine to repair acute kidney injury via AKT/Rab27 pathway. Am J Transl Res. 2021;13:1445–57.
45. Tong J, Cao L, Liu L, Jin M. Impact of autologous platelet rich plasma use on postoperative acute kidney injury in type A acute aortic dissection repair: a retrospective cohort analysis. J Cardiothorac Surg. 2021;16:9.
46. Munshi R, Johnson A, Siew ED, Ikizler TA, Ware LB, Wurfel MM, Himmelfarb J, Zager RA. MCP-1 gene activation marks acute kidney injury. J Am Soc Nephrol. 2011;22:165–75.
47. Dong Y, Siegwart DJ, Anderson DG. Strategies, design, and chemistry in SiRNA delivery systems. Adv Drug Deliv Rev. 2019;144:133–47.
48. Judge AD, Sood V, Shaw JR, Fang D, McClintock K, MacLachlan I. Sequence-dependent stimulation of the mammalian innate immune response by synthetic SiRNA. Nat Biotechnol. 2005;23:457–62.
49. Huang Y, Cheng Q, Ji JL, Zheng S, Du L, Meng L, Wu Y, Zhao D, Wang X, Lai L, et al. Pharmacokinetic behaviors of intravenously administered SiRNA in glandular tissues. Theranostics. 2016;6:1528–41.
50. Wang J, Lu Z, Wientjes MG, Au JL. Delivery of SiRNA therapeutics: barriers and carriers. AAPS J. 2010;12:492–503.
51. Gantier MP, Tong S, Behlke MA, Irving AT, Lappas M, Nilsson UW, Latz E, McMillan NA, Williams BR. Rational design of immunostimulatory SiRNAs. Mol Ther. 2010;18:785–95.
52. Tang C, Ma Z, Zhu J, Liu Z, Liu Y, Liu Y, Cai J, Dong Z. P53 in kidney injury and repair: mechanism and therapeutic potentials. Pharmacol Ther. 2019;195:5–12.
53. Paunovska K, Loughrey D, Dahlman JE. Drug delivery systems for RNA therapeutics. Nat Rev Genet. 2022;23:265–80.
54. O'Brien K, Breyne K, Ughetto S, Laurent LC, Breakefield XO. RNA delivery by extracellular vesicles in mammalian cells and its applications. Nat Rev Mol Cell Biol. 2020;21:585–606.
55. Law M, Jafari M, Chen P. Physicochemical characterization of siRNA-peptide complexes. Biotechnol Prog. 2008;24:957–63.
56. Fei SN, Ma YD, Zhou B, Chen X, Zhang Y, Yue K, Li QX, Gui YY, Xiang TY, Liu JH et al. Platelet membrane biomimetic nanoparticle-targeted delivery of TGF-β1 SiRNA attenuates renal inflammation and fibrosis. Int J Pharm. 2024;659.
57. Wei H, Chen Q, Lin L, Sha C, Li T, Liu Y, Yin X, Xu Y, Chen L, Gao W, et al. Regulation of exosome production and cargo sorting. Int J Biol Sci. 2021;17:163–77.
58. Dixson AC, Dawson TR, Di Vizio D, Weaver AM. Context-specific regulation of extracellular vesicle biogenesis and cargo selection. Nat Rev Mol Cell Biol. 2023;24:454–76.
59. Scherlinger M, Richez C, Tsokos GC, Boilard E, Blanco P. The role of platelets in immune-mediated inflammatory diseases. Nat Rev Immunol. 2023;23:495–510.

Publisher's note